*Euro. Jnl of Applied Mathematics* (2003), *vol.* 14, *pp.* 111–127.  
DOI: 10.1017/S0956792502004990 Printed in the United Kingdom

# Nucleation of vortices with a temperature and time-dependent Ginzburg–Landau model of superconductivity

E. COSKUN[1], Z. CAKIR[2] and P. TAKAC[3]

[1] *Department of Mathematics, Karadeniz Technical University, TR-61080 Trabzon, Turkey.*
[2] *Department of Mathematics, Karadeniz Technical University, TR-61080 Trabzon, Turkey.*
[3] *Department of Mathematics, University of Rostock, D-18055 Rostock, Germany.*

(*Received 11 March 1998; revised 11 February 2002*)

The standard scales that are used to non-dimensionalize the temperature- and time-dependent Ginzburg–Landau (TTDGL) model developed by Schmid [27], eliminate temperature-dependent parameters, and thus do not allow for superconducting phenomena due to variations in temperature. In this study, a set of new scales is presented to non-dimensionalize the TTDGL model so that the resulting dimensionless system depends upon a temperature parameter as well. Moreover, some properties of solutions to TTDGL system as a function of temperature are explored. Numerical experiments illustrating the temperature-dependency of vortex nucleation in type-II superconductors as well as the transition to the Meissner state in type-I superconductors are presented.

## 1 Introduction

The Ginzburg–Landau (GL) model was proposed in 1950 on phenomenological grounds, but only after the pioneering work of Abrikosov [1] and Gor'kov [17], its validity was confirmed. In 1957, Abrikosov predicted the existence of type-II superconductors based on the GL model, even before the experimental discovery of such superconductors. On the other hand, in 1959 Gor'kov was able to derive the GL model from the universally accepted microscopic BCS model under the assumptions that the temperature is sufficiently close to the critical temperature $T_c$ and the spatial variations of the order parameter and the vector potential are slow. Following these developments, the GL model has become a universally accepted macroscopic model for low-$T_c$ superconductors.

Abrikosov's work led to the classification of superconductors as type-I and type-II. The value of the GL parameter $\kappa = \frac{1}{\sqrt{2}}$ separates type-II superconductors $\left(\kappa > \frac{1}{\sqrt{2}}\right)$ from those of type-I $\left(\kappa < \frac{1}{\sqrt{2}}\right)$. This critical value arises from the equation $H_{c2} = \sqrt{2}\kappa H_c$, which relates the upper critical field $H_{c2}$ to the thermodynamical critical field $H_c$. This relation implies that for type-II superconductors $H_{c2} > H_c$, whereas for type-I superconductors $H_{c2} < H_c$. This means that a type-II superconductor may keep its superconducting features under an applied magnetic field of strength larger than $H_c$. It is this feature of type-II

superconductors that make them technologically more important, and thus attracts more attention from researchers.

High-$T_c$ superconductors, discovered by Bednorz & Müller [2], are of type-II with quite a large value of the GL parameter $\kappa$ and have rather complicated anisotropic and inhomogeneous chemical structures. The GL model has to be modified to account for high-$T_c$ superconductivity.

From a mathematical point of view, the GL system, even with some appropriate boundary conditions, does not have a unique solution. A solution to the resulting boundary value problem is not unique, unless one imposes further conditions better known as *gauge fixing*. Gauge fixing techniques resolve this problem and reduce it to a well-posed, but 'not-easy-to-handle' numerical problem, due to the nonlinear nature of the system. The numerical goal is to derive a stable scheme that can approximate possibly large gradients without destroying the gauge invariance of the system.

There has been a considerable amount of reported research work concerning a number of theoretical and numerical aspects of the GL model and its variants. Here, we do not intend to – nor can we – do a complete survey of all studies of the GL model. We name only a few that are relevant to the subject matter of our present investigation. For the physics of superconductors and the GL model, we refer to [1, 20, 21, 25]. Various results concerning the GL system and suitable finite element approximations of the solutions with natural boundary conditions are derived in Du *et al.* [10]. The GL system with periodic (or quasi-periodic) boundary conditions have been investigated [11, 22, 28]. The same problem, and its three-dimensional generalization to the Lawrence–Doniach layer model, on a much larger domain with many more vortices, were studied by Garner *et al.* [15] and Jones & Plassmann [18] using a more efficient, state-of-the-art numerical optimization and linear algebra algorithms. Kaper & Kwong [22] justified the use of the nonstandard finite difference method to solve the GL system. The simulated annealing technique was applied to the GL model in Doria *et al.* [9].

A time-dependent generalization of the stationary GL model was first derived by Schmid [27], and later justified by other physicists to study the time evolution of electromagnetic fields in low-$T_c$ superconductors subject to external effects. The model with scales that eliminate all temperature-dependent parameters, TDGL, is analyzed in Du [12], where the existence and uniqueness of weak solutions are proved, and some results concerning the regularity of solutions are provided. Various numerical schemes have been applied to TDGL [4, 6, 8, 13, 24]. An excellent survey article written for mathematicians interested in superconductivity is by Du *et al.* [10]. (See also Chan & Kwong [3].) A state-of-the-art high performance computing technology has also been effectively used in performing numerical simulations with the TDGL model; see, for example, Coskun & Kwong [5] and Galbreath [16].

The relation between the solutions of the stationary and time-dependent GL models has remained untouched for a long time. This relation was resolved by Lin & Du [23] in 1997, and investigated further by Kaper & Takac [19] in 1997.

All of the research work and related reports cited above use standard scales to non-dimensionalize the GL or TDGL equations. Unfortunately, standard scales eliminate the temperature-dependent parameters from the system and result in a model that cannot handle effects due to variations in temperature. Although the GL parameter $\kappa$ is still

temperature-dependent, it varies very slowly with the temperature so that it can be assumed to be a constant. Therefore, the resulting system does not allow any study of superconducting phenomena due to variations in temperature, even near $T_c$.

In this study, we use unconventional scales to non-dimensionalize the TDGL system so as to restore the temperature-dependence of the model by incorporating a non-dimensionalized temperature parameter into the system. The depence of the model on temperature is realized through this dimensionless parameter without having to supplement the system with any equations governing the heat transfer. Having obtained such a non-dimensionalized temperature and time-dependent GL model (TTDGL), we explore various properties of the global minimizers of the energy functional, which, of course, depends on the temperature as well. Furthermore, we modify the numerical code that we have used in our previous work [4] to perform numerical simulations for the TTDGL model. We investigate the temperature-dependency of vortex nucleation in homogeneous and isotropic thin film type-II superconductors, subject to external fields normal to the plane of the film.

The reported work concerning simulations of a mixed state with the TDGL model *for a superconductor of finite size* follows either one of the following two methods (e.g. see [3, 6, 18, 22, 24]):

- The first approach (zero-field-cooled) is to assume that a sample that is initially in a perfect superconducting state, is cooled to a temperature below the critical temperature in the absence of applied magnetic field, and then a magnetic field of an appropriate strength is suddenly turned on.
- The second approach (field-cooled) is to assume that a sample that is cooled to a temperature at or above the critical temperature is in a normal state under a magnetic field of appropriate strength, and then the temperature is suddenly decreased below the critical temperature. Furthermore, one assumes the existence of a few superconducting seeds, placed randomly across the sample, from which the nucleation process develops.

Unfortunately, neither of these approaches yields the physically meaningful global minimizer for the energy functional, where superelectron density forms a hexagonal pattern of vortices in a mixed state. Furthermore, the vortex pattern in a mixed state is often affected by the locations at which the initial seed (or seeds) are placed. See § 4 for illustrations obtained by the TDGL model.

In this study, we focus mostly on experiments performed with TTDGL system, and claim that our model yields realistic results. We assume that the sample is cooled to a critical temperature with an applied field of appropriate strength. The temperature is reduced at each step after the sample has been allowed to reach an equilibrium. In other words, at each temperature value, we let the sample equilibrate and then reduce the temperature further. We repeat the process until the model temperature reaches the value of absolute zero. In this way, we are able to observe a *natural nucleation of vortices* without having to introduce seeds from which the nucleation process develops.

This article is organized as follows. In § 2 we introduce nonstandard scales and obtain a non-dimensionalized temperature and time-dependent energy functional and TTDGL. In § 3 we provide some results concerning the minimizers of the energy functional and of TTDGL system. In § 4 we illustrate graphically the results of numerical simulations which

were performed on an Intel-based workstation located at the Department of Informatics, Karadeniz Technical University.

## 2 TTDGL model in non-dimensional units

### 2.1 TTDGL energy functional in non-dimensional units

First we consider the free energy functional [1]

$$F(\Psi,\mathbf{A})=\int_{\Omega}\left(\alpha(T)|\Psi|^2+\frac{\beta(T)}{2}|\Psi|^4+\right.$$
$$\left.\frac{1}{2m^*}\left|\left(\frac{\hbar}{i}\nabla-\frac{e^*}{c}\mathbf{A}\right)\Psi\right|^2+\frac{|\nabla\times\mathbf{A}|^2}{8\pi}-\frac{\nabla\times\mathbf{A}}{4\pi}\cdot\mathbf{H}_0\right)d\Omega, \tag{2.1}$$

where $e^*$ and $m^*$ are effective values of the mass and charge of the superconducting electrons, $c$ is the speed of light, $\Psi$ is the complex-valued order parameter, $\mathbf{A}$ is the magnetic vector potential, $\mathbf{H}_0$ is the applied magnetic field, $T$ is the temperature and $\Omega$ is the domain occupied by the superconductor. Here $\alpha(T)$ changes sign at $T=T_c$, the critical temperature. More precisely $\alpha(T)<0$ for $T<T_c$ and $\alpha(T)>0$ for $T>T_c$, and $\beta(T)>0$ for all $T$.

Based on empirical approximations [26],

$$\alpha(\tau)=(\tau-1)\alpha_0(\tau), \tag{2.2}$$

where

$$\alpha_0(\tau)=\alpha(0)\frac{\tau+1}{\tau^2+1},\quad \alpha(0)=-\frac{e^{*2}}{m^*c^2} \tag{2.3}$$

and $\tau=\frac{T}{T_c}$. Also,

$$\beta(\tau)=\frac{\beta(0)}{(1+\tau^2)^2},\ \beta(0)=\frac{4\pi e^{*4}}{m^{*2}c^4}. \tag{2.4}$$

Now, we let

$$|\bar{\Psi}_0|^2=\frac{\alpha_0}{\beta},\quad \bar{\lambda}=\left(\frac{m^*}{4\pi|\bar{\Psi}_0|^2}\right)^{1/2}\frac{c}{e^*},\quad \bar{H}_0=\left(4\pi\alpha_0|\bar{\Psi}_0|^2\right)^{1/2}$$

and

$$\bar{\xi}=\left(\frac{\hbar^2}{2m^*\alpha_0}\right)^{1/2}.$$

We make the following substitutions:

$$\mathbf{x}'=\frac{\mathbf{x}}{\bar{\lambda}},\quad \Psi'=\frac{\Psi}{\bar{\Psi}_0},\quad \mathbf{A}'=\frac{1}{\bar{\lambda}\bar{H}_0\sqrt{2}}\mathbf{A},\ \mathbf{H}_0'=\frac{\mathbf{H}_0}{\sqrt{2}\bar{H}_0},\quad F'(\Psi',\mathbf{A}')=\frac{F(\Psi,\mathbf{A})}{\alpha_0|\bar{\Psi}_0|^2}.$$

Then we have

$$\alpha|\Psi|^2+\frac{\beta}{2}|\Psi|^4=\alpha_0|\bar{\Psi}_0|^2\left[(\tau-1)|\Psi'|^2+\frac{1}{2}|\Psi'|^4\right]. \tag{2.5}$$

We note that

$$\frac{e^*}{c}\bar{\lambda}\bar{H}_0\sqrt{2}\mathbf{A}'=(m^*)^{1/2}\alpha_0^{1/2}\sqrt{2}\mathbf{A}',$$

https://doi.org/10.1017/S0956792502004990 Published online by Cambridge University Press

so that the kinetic energy term can be written as

$$\begin{aligned}
\frac{1}{2m^*}\left|\left(\frac{\hbar}{i}\nabla-\frac{e^*}{c}\mathbf{A}\right)\Psi\right|^2 &= \frac{1}{2m^*}\left|\left(\frac{\hbar}{i}\frac{1}{\bar{\bar{\lambda}}}\nabla-\frac{e^*}{c}\bar{\lambda}\bar{H}_0\sqrt{2}\mathbf{A}'\right)\Psi'\bar{\Psi}_0\right|^2 \\
&= \left|\left(\frac{\hbar}{i\sqrt{2m^*}\bar{\lambda}}\nabla-\alpha_0^{1/2}\mathbf{A}'\right)\Psi'\bar{\Psi}_0\right|^2 \\
&= |\bar{\Psi}_0|^2\alpha_0\left|\left(\frac{\hbar}{i\sqrt{2m^*\alpha_0}\bar{\lambda}}\nabla-\mathbf{A}'\right)\Psi'\right|^2 \\
&= |\bar{\Psi}_0|^2\alpha_0\left|\left(\frac{1}{i}\frac{\bar{\bar{\xi}}}{\bar{\lambda}}\nabla-\mathbf{A}'\right)\Psi'\right|^2 \\
&= |\bar{\Psi}_0|^2\alpha_0\left|\left(\frac{1}{\kappa i}\nabla-\mathbf{A}'\right)\Psi'\right|^2.
\end{aligned}$$

In the last equality above, we have used the fact that

$$\bar{\kappa}=\frac{\bar{\lambda}}{\bar{\bar{\xi}}}=\frac{\lambda}{\xi}=\kappa,$$

which follows immediately from the definition of the GL parameter, $\kappa=\frac{\lambda}{\xi}$, where

$$\lambda=\left(\frac{m^*}{4\pi|\Psi_0|^2}\right)^{1/2}\frac{c}{e^*},\ \xi=\left(\frac{\hbar^2}{2m^*|\alpha|}\right)^{1/2}\text{ and }|\Psi_0|^2=\frac{\alpha}{\beta}.$$

Similarly, it can easily be shown that

$$\frac{|\nabla\times\mathbf{A}|^2}{8\pi}=\alpha_0|\bar{\Psi}_0|^2|\nabla\times\mathbf{A}'|^2$$

and finally,

$$\frac{\nabla\times\mathbf{A}}{4\pi}\cdot\mathbf{H}_0=2\alpha_0|\bar{\Psi}_0|^2(\nabla\times\mathbf{A}')\cdot\mathbf{H}_0'.$$

Now we drop the primes and non-dimensionalize the free energy by $\alpha_0|\bar{\Psi}_0|^2$, and consider the equality

$$|\nabla\times\mathbf{A}|^2-2(\nabla\times\mathbf{A})\cdot\mathbf{H}_0=|\nabla\times\mathbf{A}-\mathbf{H}_0|^2-|\mathbf{H}_0|^2,$$

from which we ignore the contribution of the term $-|\mathbf{H}_0|^2$ to the free energy, and thus obtain

$$F_\tau(\Psi,\mathbf{A})=\int_\Omega\left[(\tau-1)|\Psi|^2+\frac{1}{2}|\Psi|^4+\left|\left(\frac{1}{\kappa i}\nabla-\mathbf{A}\right)\Psi\right|^2+|\nabla\times\mathbf{A}-\mathbf{H}_0|^2\right]d\Omega,$$

where the $\tau$-dependence of $\kappa$ and $\mathbf{H}_0$ is given above.

### 2.2 Temperature and time-dependent GL (TTDGL)

Based on Schmid's derivation, TTDGL can be formulated as

$$\eta\left(\frac{\partial}{\partial t}+i\kappa\phi\right)\Psi=-\frac{\delta F_\tau}{\delta\Psi^*},\tag{2.6}$$

$$\left(\frac{\partial\mathbf{A}}{\partial t}+\nabla\phi\right)=-\frac{1}{2}\frac{\delta F_\tau}{\delta\mathbf{A}},\tag{2.7}$$

https://doi.org/10.1017/S0956792502004990 Published online by Cambridge University Press

which holds in $\Omega \times (0, \infty)$, where $\phi$ denotes scalar electric potential, and $\eta$ is a relaxation parameter. For simplicity, we take $\eta = 1$. The model is invariant under the Gauge transformation

$$F_\chi(\Psi, \mathbf{A}, \phi) = (\Psi', \mathbf{A}', \phi'),$$

where

$$\Psi' = \Psi e^{\kappa\chi}, \quad \mathbf{A}' = \mathbf{A} + \nabla\chi, \quad \phi' = \phi - \frac{\partial\chi}{\partial t}.$$

There are various admissible gauge choices. One can choose an admissible gauge to suit the aspect of the model being investigated. For numerical computations, the so-called zero potential gauge is more convenient. This gauge is defined to be the solution of the system [12]

$$\frac{\partial\chi}{\partial t} = \phi,$$

and at $t = 0$, $\Delta\chi = -\text{div}\mathbf{A}$ in $\Omega$ with $\nabla\chi \cdot \mathbf{n} = -\mathbf{A} \cdot \mathbf{n}$ on $\Gamma$, where $\mathbf{n}$ denotes the unit normal vector of the boundary $\Gamma$ of $\Omega$.

In this gauge, the electric potential is eliminated from the system. Thus, applying the gauge transformation to the TTDGL system and dropping the primes, the TTDGL becomes

$$\frac{\partial\Psi}{\partial t} = -\frac{\delta F_\tau}{\delta\Psi^*}, \quad \frac{\partial\mathbf{A}}{\partial t} = -\frac{1}{2}\frac{\delta F_\tau}{\delta\mathbf{A}}.$$

In explicit form,

$$\frac{\partial\Psi}{\partial t} = \left((1-\tau) - |\Psi|^2\right)\Psi - \left(\frac{i}{\kappa}\nabla + \mathbf{A}\right)^2\Psi, \tag{2.8}$$

$$\frac{\partial\mathbf{A}}{\partial t} = -\nabla \times \nabla \times \mathbf{A} + \frac{1}{2\kappa i}(\Psi^*\nabla\Psi - \Psi\nabla\Psi^*) + \mathbf{A}|\Psi|^2 \tag{2.9}$$

with the so-called natural boundary conditions

$$\left(\frac{i}{\kappa}\nabla + \mathbf{A}\right)\Psi \cdot \mathbf{n} = 0, \tag{2.10}$$

$$(\nabla \times \mathbf{A}) \times \mathbf{n} = \mathbf{H}_0 \times \mathbf{n} \quad \text{on} \quad \Gamma \times (0, \infty). \tag{2.11}$$

The first condition implies that no supercurrent can flow throughout the sample, and the second condition expresses that the normal component of the induced magnetic field is continuous across the boundary. Furthermore, the TTDGL system at $\tau = 1$, the initial temperature, has to be supplemented with initial conditions

$$\Psi(\mathbf{x}, \mathbf{0}) = \Psi_0(\mathbf{x}), \quad \mathbf{A}(\mathbf{x}, \mathbf{0}) = \mathbf{A_0}(\mathbf{x}). \tag{2.12}$$

In the zero electric potential gauge, we have div $\mathbf{A}_0(\mathbf{x}) = \mathbf{0}$ and $\mathbf{A}_0(\mathbf{x}) \cdot \mathbf{n} = 0$. Moreover, we make a physically meaningful assumption that $|\Psi_0(\mathbf{x})| \leqslant 1$. This condition implies that at the critical temperature the magnitude of the initial order parameter does not exceed its value at the superconducting state at temperature absolute zero.

https://doi.org/10.1017/S0956792502004990 Published online by Cambridge University Press

## 3 Results concerning the solution of TTDGL and minimizers of $F_\tau(\Psi, \mathbf{A})$

Let $H^1(\Omega)$ [$\mathbf{H}^1(\Omega)$] denote the Sobolev space of real [*vector*] valued functions having square integrable derivatives of order 1, $\mathscr{H}^1(\Omega)$ denote the corresponding space of complex-valued functions. We have the following properties of the temperature-dependent GL energy functional $F_\tau(\Psi, \mathbf{A})$, which are the extensions of the results presented in Du *et al.* [11] to the temperature-dependent model.

First, we point out that the functional $F_\tau$ has the gauge invariant property, i.e. for any real-valued smooth function $\chi$,

$$F_\tau(\Psi e^{i\chi}, \mathbf{A} + \nabla\chi) = F_\tau(\Psi, \mathbf{A}).$$

Next, we have the following property.

**Proposition 3.1** *For* $0 \leqslant \tau \leqslant 1$, *if* $\mathbf{H}_0 = \mathbf{0}$ *then* $\Psi = \sqrt{1-\tau}$ *and* $\mathbf{A} = \mathbf{0}$ *is the global minimizer of* $F_\tau(\Psi, \mathbf{A})$.

**Proof** Let us rewrite $F_\tau(\Psi, \mathbf{A})$ as

$$F_\tau(\Psi, \mathbf{A}) = \int_\Omega \left[ \frac{1}{2}\left(|\Psi|^2 + (\tau - 1)\right)^2 + \left| \left( \frac{1}{\kappa i}\nabla - \mathbf{A} \right) \Psi \right|^2 + |\nabla \times \mathbf{A} - \mathbf{H}_0|^2 - \frac{1}{2}(\tau - 1)^2 \right] d\Omega.$$

Then it is easily seen that

$$F_\tau(\Psi, \mathbf{A}) \geqslant F_\tau(\sqrt{1-\tau}, 0) = -\frac{1}{2}(\tau - 1)^2 meas(\Omega)$$

for all $(\Psi, \mathbf{A}) \in \mathscr{H}^1(\Omega) \times \mathbf{H}^1(\Omega)$. Equality holds if and only if $\Psi = \sqrt{1-\tau}$ and $\mathbf{A} = \mathbf{0}$. We note that this minimizer is unique up to a constant gauge. □

**Remark 3.2** *We note that* $\tau = 1$ *corresponds to the critical temperature. So it follows from Proposition 3.1 that when* $\mathbf{H}_0 = \mathbf{0}$, *then the zero solution is the only global minimizer. We also note that if* $\Psi = 0$, *then the steady GL system corresponding to* (2.8)–(2.9) *reduces to*

$$\nabla \times \nabla \times \mathbf{A} = \mathbf{0} \text{ in } \Omega \tag{3.1}$$

$$(\nabla \times \mathbf{A} - \mathbf{H}_0) \times \mathbf{n} = \mathbf{0} \text{ on } \Gamma. \tag{3.2}$$

**Proposition 3.3** *For any* $\mathbf{H}_0 \neq \mathbf{0}$, *if* $\tilde{\mathbf{A}}$ *is a solution of* (3.1)–(3.2) *then the pair* $(\Psi, \mathbf{A}) = (0, \tilde{\mathbf{A}})$ *is the global minimizer of* $F_1(\Psi, \mathbf{A})$ *up to any smooth gauge.*

**Proof** It follows from the fact that

$$F_1(0, \tilde{\mathbf{A}}) = 0 <= F_1(\Psi, \mathbf{A})$$

for all $(\Psi, \mathbf{A}) \in \mathscr{H}^1(\Omega) \times \mathbf{H}^1(\Omega)$. □

**Proposition 3.4** *Let* $h_s = sup_\Omega |\mathbf{H}_0|$. *For any* $\tau \in [0, 1)$, *if* $h_s < \frac{1}{\sqrt{2}}(1 - \tau)$ *then the solution*

https://doi.org/10.1017/S0956792502004990 Published online by Cambridge University Press

$(0, \tilde{\mathbf{A}})$ *cannot be a global minimizer. Likewise, if* $h_s > \frac{1}{\sqrt{2}}(1-\tau)$ *then the solution* $(\sqrt{1-\tau}, \mathbf{0})$ *cannot be global minimizer, where* $\tilde{\mathbf{A}}$ *is a solution of the system* (3.1)–(3.2).

**Proof** Note that $F_\tau(0, \tilde{\mathbf{A}}) = 0$ and $F_\tau(\sqrt{1-\tau}, 0) = (-\frac{1}{2}(1-\tau)^2 + |\mathbf{H}_0|^2) meas(\Omega)$. So if $h_s < \frac{1}{\sqrt{2}}(1-\tau)$ then $F_\tau(\sqrt{1-\tau}, \mathbf{0}) < F_\tau(0, \tilde{\mathbf{A}})$. Therefore, the normal solution can not be a global minimizer. The rest of the proposition follows similarly. □

**Remark 3.5** *If* $|\mathbf{H}_0| = \frac{1}{\sqrt{2}}(1-\tau)$ *then* $F_\tau(0, \tilde{\mathbf{A}}) = F_\tau(\sqrt{1-\tau}, 0)$. *So in terms of the scales used in this study, the thermodynamical critical field is* $H_c = \frac{1}{\sqrt{2}}(1-\tau)$. *Based on the approximations given in Tinkham* [26], *we have* $H_{c1} = \frac{1}{2\kappa}(1-\tau)$, *and* $H_{c2} = \kappa(1-\tau)$.

For the TDGL, the following result for the order parameter has been proved in Du [12] (Lemma 3.7) for the weak formulation of the TDGL system in the zero potential gauge.

**Proposition 3.6** *(* Du [12] Lemma 3.7) *If* $(\Psi(t), \mathbf{A}(t))$ *is a solution of TDGL system and if* $|\Psi_0(\mathbf{x})| \leqslant 1$ *a.e. in* $\Omega$ *then* $|\Psi(\mathbf{x}, t)| \leqslant 1$ *a.e.,* $\forall (\mathbf{x}, t) \in \Omega \times [0, T]$.

In what follows, we give the analogue of this bound for TTDGL.

**Proposition 3.7** *If* $(\Psi(t), \mathbf{A}(t))$ *is a solution of TTDGL system for a fixed* $\tau \in [0, 1]$ *and if* $|\Psi_0(\mathbf{x})| \leqslant \sqrt{1-\tau}$ *a.e. in* $\Omega$ *then* $|\Psi(\mathbf{x}, t)| \leqslant \sqrt{1-\tau}$ *a.e.,* $\forall (\mathbf{x}, t) \in \Omega \times [0, T]$.

**Proof** The proof follows easily from that of Proposition 3.6 given in Du [12]. □

**Corollary 3.8** *The TTDGL system at* $T = T_c$ *reduces to*

$$\frac{\partial \Psi}{\partial t} = -|\Psi|^2 \Psi - \left(\frac{i}{\kappa i}\nabla + \mathbf{A}\right)^2 \Psi,$$
$$\frac{\partial \mathbf{A}}{\partial t} = -\nabla \times \nabla \times \mathbf{A} + \frac{1}{2\kappa i}(\Psi^* \nabla \Psi - \Psi \nabla \Psi^*) - |\Psi|^2 \mathbf{A}$$

*which has no solution with* $\Psi \neq 0$ *and with* $\Psi_0(\mathbf{x}) = \mathbf{0}$.

**Proof** Follows immediately from Proposition 3.7. □

**Proposition 3.9** *If* $(\Psi, \mathbf{A})$ *is a solution of TTDGL for any* $\tau$ *then the inequality*

$$||\Psi(t)||_{L^2}^2 \leqslant ||\Psi_0||_{L^2}^2 e^{2(1-\tau)\int_0^t ||\Psi(s)||_{L^2}^2 ds}$$

*holds* $\forall\, t \geqslant 0$.

**Proof** From (2.8) we see that

$$\frac{\partial}{\partial t}(\Psi \Psi^*) = -\Psi^* \left(\frac{i}{\kappa}\nabla + \mathbf{A}\right)^2 \Psi - \Psi \left(\frac{i}{\kappa}\nabla - \mathbf{A}\right)^2 \Psi^*$$
$$+ 2(-|\Psi|^4 + (1-\tau)|\Psi|^2)$$

https://doi.org/10.1017/S0956792502004990 Published online by Cambridge University Press

$$= \frac{1}{\kappa^2}\Delta(\Psi\Psi^*) - 2\left|\frac{i}{\kappa}\nabla + \mathbf{A}\Psi\right|^2$$
$$- 2(-|\Psi|^4 + (1-\tau)|\Psi|^2)$$
$$\leqslant \frac{1}{\kappa^2}\Delta(\Psi\Psi^*) + 2(1-\tau)|\Psi|^2. \tag{3.3}$$

On the other hand, the boundary condition (2.10) implies that

$$\int_\Omega \Delta|\Psi|^2 d\mathbf{x} = \int_\Omega \nabla|\Psi|^2 \cdot \mathbf{n} d\sigma(\mathbf{x}) = 0. \tag{3.4}$$

Integrating (3.3) over $\Omega$ and using (3.4), we get

$$\frac{\partial}{\partial t}||\Psi||_{L^2}^2 \leqslant 2(1-\tau)||\Psi||_{L^2}^2. \tag{3.5}$$

Finally, use of Gronwall's inequality in (3.5) completes the proof. □

**Corollary 3.10** *For any $\tau > 1$, if $(\Psi(t), \mathbf{A}(t))$ is a nontrivial solution of the TTDGL then $(\psi(t), \mathbf{A}(t)) \to (0, \tilde{\mathbf{A}})$ as $t \to \infty$.*

In what follows, we investigate numerically some electromagnetic properties of superconductors with the TTDGL. In particular, we study vortex patterns in equilibrium state with both TDGL and TTDGL, and relate the results to those of physical experiments.

## 4 Numerical experiments

We consider a finite homogeneous superconducting film of uniform thickness, subject to a constant external magnetic field normal to the plane of the film. In this setting, the vector potential can be viewed as $\mathbf{A} = (A, B, 0)$, and the model becomes two-dimensional.

Before discretizing the TTDGL, we introduce the so-called bond variables (e.g. see Kwong & Kaper [22])

$$W(x,y) = e^{i\kappa\int^x A(\zeta,y)d\zeta}, \quad V(x,y) = e^{i\kappa\int^y B(x,\eta)d\eta}$$

into the system so that the discretized system can be gauge-invariant as well. We use the same discretization technique that we have used in our previous works [6, 8] to spatially discretize this system and employ the Forward Euler method for temporal discretization. We could use the Modified Forward Euler (MFE) method, which we introduced earlier [6], but the MFE method requires the storage of data from a previous step, and thus limits the size of the problem we may investigate.

For all the experiments with TDGL, we assume that the samples are of a size $250\lambda \times 250\lambda$, and subject to an applied magnetic field $\mathbf{H}_0 = (0, 0, H)$ of strength $H = 1$.

### 4.1 Experiments with TDGL

In what follows we present experiments to justify our claim that the vortex pattern, obtained through TDGL, in the equilibrium state depends strongly upon initial conditions. Namely, we provide two typical experiments for the *field-cooled* and *zero-field-cooled* processes, and observe that they do not yield the same vortex configuration on samples

https://doi.org/10.1017/S0956792502004990 Published online by Cambridge University Press

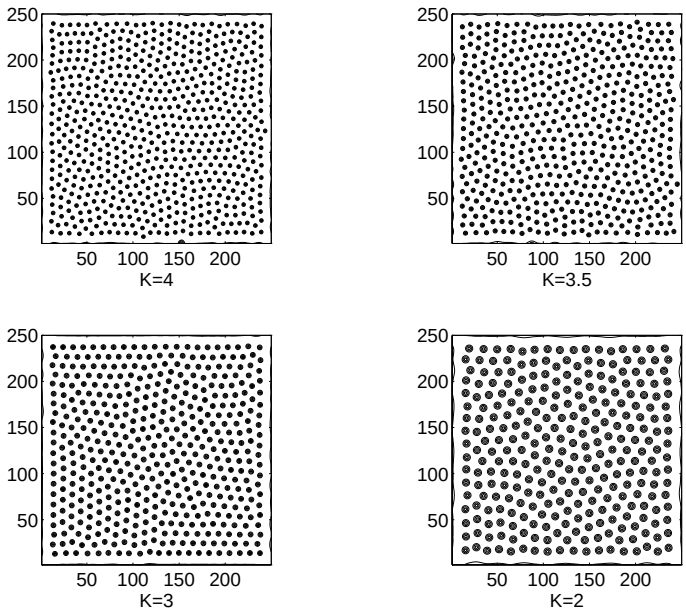


FIGURE 1. Vortex nucleation in the zero-field-cooled process.

with *identical* physical properties and subject to the *same* external effects. Moreover, neither process yields the physically meaningful hexagonal vortex pattern with the TDGL system.

### 4.1.1 *Experiment I (Zero-field-cooled process with TDGL)*

In this experiment we simulate the physical process, the so-called *zero-field-cooling*. More precisely, we assume that the sample, which is initially in a perfect superconducting state, is cooled through $T_c$ in the absence of applied magnetic field, and then a magnetic field of an appropriate strength is suddenly turned on. In mathematical terms, the initial state is achieved by letting $|\Psi_0(\mathbf{x})| = 1$, $\mathbf{A}_0(\mathbf{x}) = \mathbf{0}$ for all $\mathbf{x} \in \Omega$. In Figure 1, we show a contour plot of superelectron density corresponding to samples with GL parameters $\kappa = 4, 3.5, 3, 2$. A careful examination of the results reveals a *partial hexagonal pattern* depending on the value of $\kappa$, yet we do not observe the physically meaningful exact hexagonal pattern, as expected of homogeneous samples with uniform thickness.

### 4.1.2 *Experiment II (Field-cooled process with TDGL)*

In this experiment, we simulate the *field-cooled* process. We assume that the sample, which is cooled to a temperature at or above the critical temperature, is in a normal state under a magnetic field of appropriate strength, and then the temperature is suddenly reduced to below $T_c$. In mathematical terms, the initial state is achieved by letting

$$\mathbf{A}_0(x,y) = (0, xH, 0)\,, \quad \Psi_0(x,y) = \begin{cases} 0 & \text{if} \quad (x,y) \neq (x_0,y_0) \\ c & \text{if} \quad (x,y) = (x_0,y_0) \end{cases},$$

https://doi.org/10.1017/S0956792502004990 Published online by Cambridge University Press

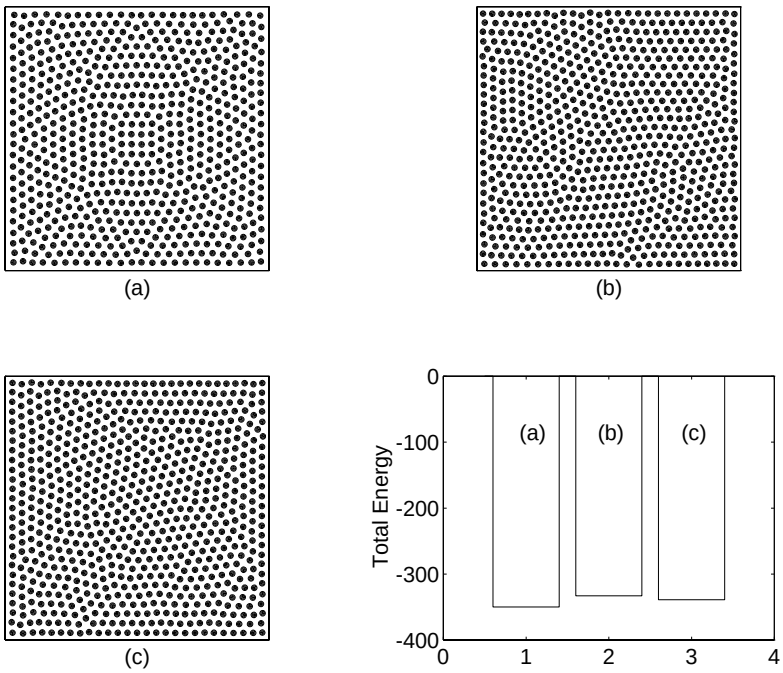


FIGURE 2. Vortex nucleation in the field-cooled process with seeds.

where $c > 0$ is a small constant representing the magnitude of the seed, and $(x_0, y_0)$ is the location of a seed in the sample. By carrying out many experiments, we came to the conclusion that the resulting vortex pattern depends upon where and how many seeds are placed into the sample. Some numerical results, typical of our findings, are illustrated in Figures 2(a), (b) and (c), corresponding to a single seed located at $(x_0, y_0) = (125\lambda, 125\lambda), (50\lambda, 25\lambda), (63\lambda, 63\lambda)$, respectively. The magnitude of the seed, $c$ is set to 0.01. Depending on where the initial seed is placed, the energy functional assumes different values which is also illustrated in Figure 2. The lowest energy value is attained for the seed located at the center of the sample (Figure 2(a)), which results in a symmetrical vortex pattern with respect to the diagonals. The symmetry is broken for the other two cases.

### 4.2 Experiments with TTDGL

In the experiments below, first we solve the TTDGL system for type-II superconductors of small and large sizes subject to applied magnetic field of strength $|\mathbf{H}_0| = 1$. In Experiments III and IV, we illustrate graphically nucleation of vortices as the temperature parameter approaches absolute zero. Finally, in Experiment V we solve the TTDGL system for a type-I superconductor and illustrate graphically transition to the Meissner state as the temperature approaches absolute zero. We begin with the nucleation procedure that we use in Experiments III and IV.

https://doi.org/10.1017/S0956792502004990 Published online by Cambridge University Press

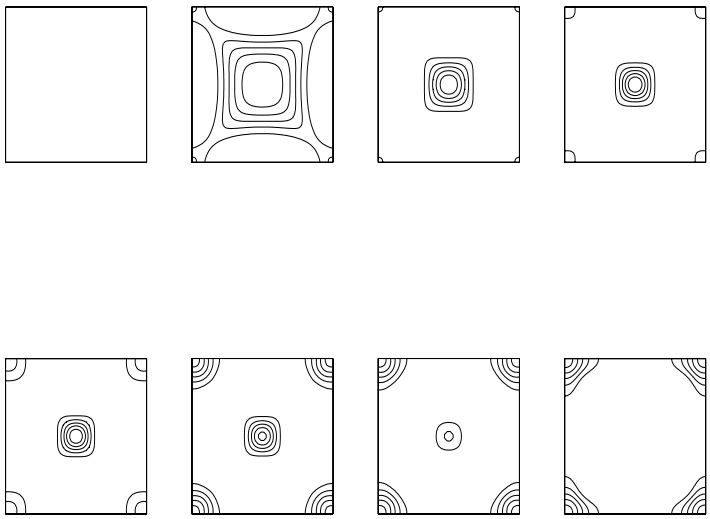

FIGURE 3. Nucleation procedure with TTDGL at $\tau = 1$.

4.2.1 *Nucleation procedure with TTDGL*

We assume that the sample is placed at the critical temperature, $\tau = 1$, in the absence of applied magnetic field and then a magnetic field of appropriate strength is turned on. We make a physically meaningful assumption that the magnitude of the initial order parameter does not exceed its value at the superconducting state at temperature absolute zero and let the sample equilibreate as the time parameter $t(\tau) \to t_e(\tau)$, where $t_e(\tau)$ is the time at which the sample reaches at the equilibrium state for a particular $\tau$ which ranges from 1 to 0. The initial state is achieved with the conditions $|\Psi_0(\mathbf{x})| = c \leqslant 1$, $\mathbf{A}_0(\mathbf{x}) = \mathbf{0}$ for all $\mathbf{x} \in \Omega$. In Figure 3, we illustrate graphically the transition to the equilibrium state as $t(1) \to t_e(1)$. The contours represent the magnitute of order parameter. We observe that as a magnetic field of strength $|\mathbf{H}_0| = \mathbf{1}$ is applied to the sample, a phase shift towards the normal state occurs. We note that the contour levels for the pictures in bottom row are of order $10^{-10}(left) \to 10^{-18}(right)$. As we proceed the relaxation procedure no discernable change within the computational precisions takes place, therefore the final state represented in the last picture of the second row in Figure 3 is assumed to be an initial state for the next stage of the nucleation procedure which assumes a smaller value of $\tau$.

In this way, the nucleation procedure we follow goes through a natural temporal and thermal evolution. Thus, no seeding procedure is needed to initiate the nucleation.

4.2.2 *Experiment III (Vortex nucleation for a sample of small size with TTDGL)*

In this experiment, we consider a type-II superconductor of size $50\lambda \times 50\lambda$ with $\kappa = 4$ and $\mathbf{H}_0 = (0, 0, H), H = 1$. We assume that the sample is placed at a critical temperature, i.e. $\tau = 1$. The nucleation procedure is the same as outlined above. The value of $\tau$ is reduced by 1% at each step after the sample is allowed to reach equilibrium. More precisely, at each temperature we let the sample equilibrate, and then reduce temperature by 1%, and

https://doi.org/10.1017/S0956792502004990 Published online by Cambridge University Press

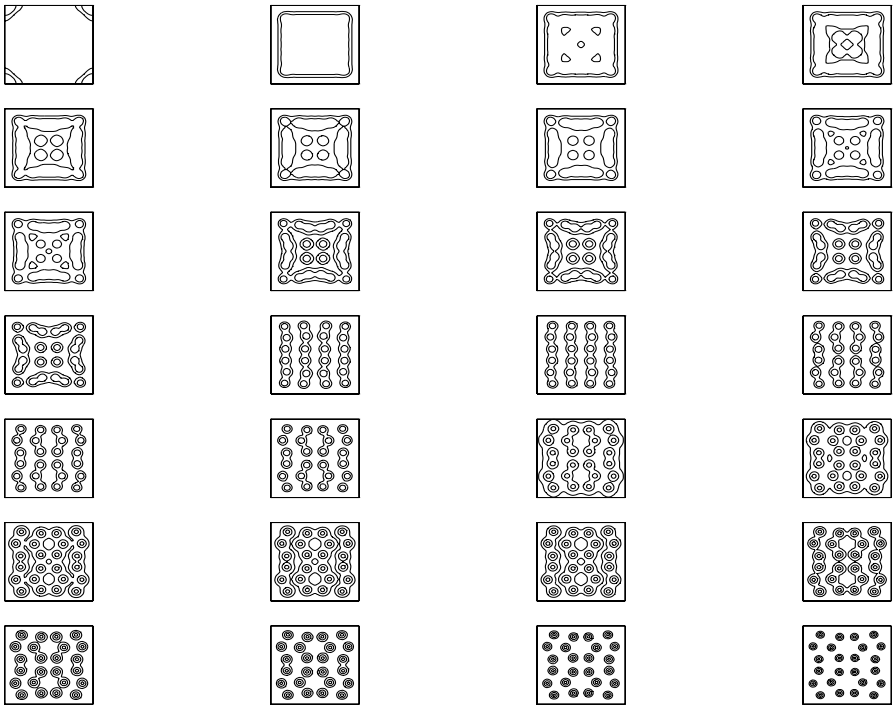

FIGURE 4. Vortex nucleation with TTDGL for a sample of size $50\lambda \times 50\lambda$.

repeat the process until the temperature reaches at the absolute zero. The contour plot of superelectron density corresponding to 28 different temperature values are illustrated in Figure 4 with contour levels at $(mpsi/4, mpsi/2, mpsi)$ for the top 18 pictures, and with contour levels at (0.1,0.3,0.5) for the remaining 10 pictures, where $mpsi = \max_{\Omega} |\Psi|$. The pictures illustrated in Figure 4 correspond to the selected temperature values:

$$\tau = \begin{bmatrix} 0.80 & 0.74 & 0.71 & 0.70 \\ 0.69 & 0.68 & 0.67 & 0.65 \\ 0.64 & 0.57 & 0.55 & 0.52 \\ 0.51 & 0.50 & 0.49 & 0.47 \\ 0.45 & 0.42 & 0.40 & 0.36 \\ 0.33 & 0.32 & 0.31 & 0.25 \\ 0.20 & 0.17 & 0.10 & 0.00 \end{bmatrix}.$$

The values are chosen so that the dynamics of vortex nucleation can be followed easily as the temperature approaches to absolute zero.

As a final equilibrium state, we observe two hexagonal chains of vortices. Next, we illustrate the graphical results obtained for a larger size of a type-II superconductor.

### 4.2.3 *Experiment IV (Vortex nucleation for a sample of large size with TTDGL)*

In this experiment, we consider a type-II superconductor of size $250\lambda \times 250\lambda$ with $\kappa = 3$ and $\mathbf{H}_0 = (0,0,H)$,$H$=1. The contour plot of superelectron density correspond-

https://doi.org/10.1017/S0956792502004990 Published online by Cambridge University Press

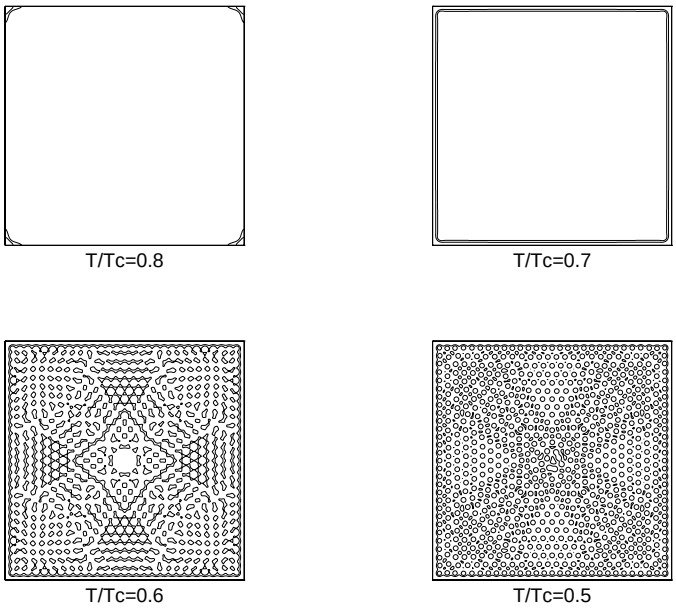


FIGURE 5. Vortex nucleation with TTDGL.

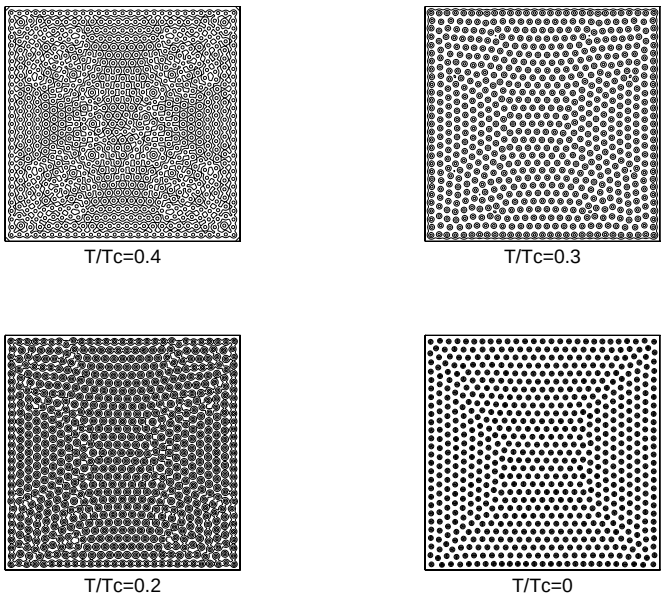


FIGURE 6. Vortex nucleation with TTDGL (continued).

ing to four different temperature values are illustrated in Figure 5 with contour levels at $(mpsi/4, mpsi/2, mpsi)$, where $mpsi = \max_{\Omega} |\Psi|$, and Figure 6 with contour levels at (0.1,0.3,0.5). Set initially at a critical temperature with the the nucleation procedure outlined above, first the sample equilibrates to the *normal state,* and then we observe the nucleation of vortices as the temperature parameter is being reduced. Nucleation starts

https://doi.org/10.1017/S0956792502004990 Published online by Cambridge University Press

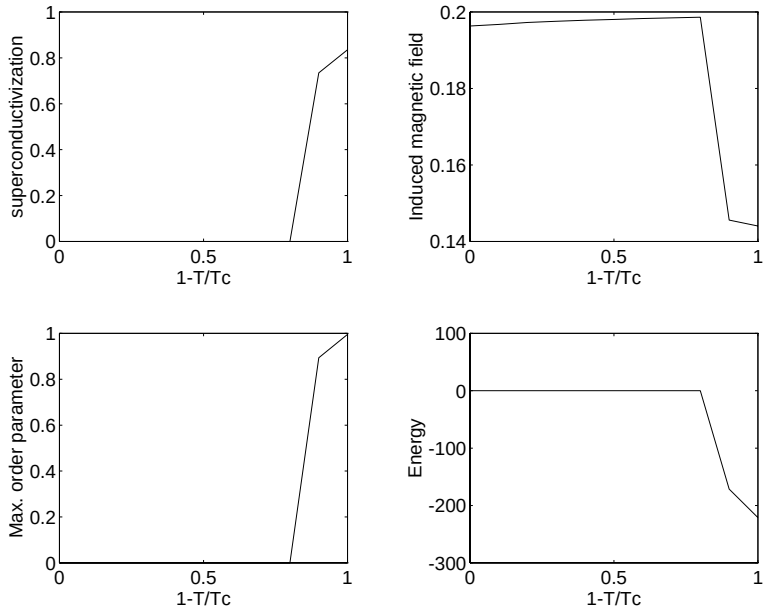


FIGURE 7. Transition to the Meissner state as $\mathrm{T/Tc} \to \mathbf{0}$.

initially at the corners and subsequently spreads out across the whole sample. The final state which corresponds to $\tau = 0$ is composed of *hexagonal patterns*, as expected of a homogeneous type-II superconductor of uniform thickness.

We observe that the transition from normal to a mixed state occurs suddenly at around $T/T_c = 0.6$.

### 4.2.4 *Experiment V (Transition to the Meissner state with TTDGL)*

In this experiment, we consider a type-I superconductor of the size same as above with $\kappa = 0.7, |\mathbf{H}_0| = 0.2$, and observe the transition to the Meissner state, i.e. the exclusion of induced magnetic flux as the sample cools down to a temperature below $T_c$.

To measure the rate at which the material, initially in normal state, enters the mixed state we introduce a term, the so-called *superconductivization*, and define it as

$$S(t) = \frac{1}{|\Omega|} \int_{\Omega} |\Psi|^2 d\Omega,$$

and also we look at the overall magnetization,

$$M(t) = \frac{1}{|\Omega|} \int_{\Omega} |\nabla \times \mathbf{A}| d\Omega$$

$\forall t \geqslant 0$. We illustrate in Figure 7 the quantities: superconductivization, magnetization, maximum of order parameter, and energy functional as temperature parameter decreases from $T_c$ to 0.

To the best of our knowledge, this is the first experiment with the two-dimensional

https://doi.org/10.1017/S0956792502004990 Published online by Cambridge University Press

TDGL system, simulating the transition to the Meissner state as a function of temperature. Notice, as known physically, how sharp the transition takes place.

## 5 Conclusion

The temperature- and time-dependent GL system, originally developed by Schmid, is non-dimensionalized using a new set of scales so as to preserve the temperature dependency. Some properties of the resulting temperature dependent energy functional and of the solution to TTDGL system are presented. Furthermore, we perform numerical experiments with the TDGL system, which does not include a temperature-dependent parameter, justifying our claim that the vortex configuration in the mixed state depends upon initial state of the sample and that the system does not seem to yield hexagonal pattern for finite size homogeneous samples of uniform thickness with the natural boundary conditions. On the other hand, the TTDGL system leads to the expected hexagonal pattern, i.e. the global minimizer of the energy functional. However, the simulation process with the TTDGL system requires much more, almost ten fold, cpu time as compared to that required for the classical TDGL system.

## Acknowledgements

The first author gratefully acknowledges the scholarship provided by Turkish and German research societies, TUBITAK and DFG, which helped realize his visit to Rostock University for a period of two month, where this research has been initiated and the funding provided by Karadeniz Technical University under project #21.111.003.1.

## References

[1] Abrikosov, A. A. (1998) *Fundamentals of the Theory of Metals*. Elsevier Science.
[2] Bednorz, J. G. & Müller, K. A. (1986) Possible high-$T_c$ super conductivity in the Ba-La-Cu-O system. *Z. Phys. B*, **64**, 189.
[3] Chan, C. Y. & Kwong, M. K. (1993) *Proceedings Nonlinear Problems in Superconductivity: First World Congress of Nonlinear Analysists*, Argonne National Laboratory, Argonne, IL.
[4] Coskun, E. (1994) *Numerical analysis of Ginzburg-Landau models for superconductivity*. PhD Dissertation, Northern Illinois University, DeKalb, IL.
[5] Coskun, E. & Kwong, M. K. (1995) Parallel solution of the time-dependent Ginzburg-Landau equations. *Technical report, MCS, ANL-95/49*, Argonne National Laboratory, Argonne, IL.
[6] Coskun, E. & Kwong, M. K. (1997) Simulating vortex motion in superconducting films with the time-dependent Ginzburg-Landau equations. *Nonlinearity* **10**, 579–593.
[7] Coskun, E. (1997) On some bounds for the solutions of the time-dependent Ginzburg-Landau equations. *Turkish J. Math.* **21**, 25–44.
[8] Coskun, E. (1999) Computational simulation of flux trapping and vortex pinning in type-II superconductors. *Appl. Math. Comput*. **106**, 31–49.
[9] Doria, M., Gubernatis, J. & Rainer, D. (1990) Solving the Ginzburg-Landau equations by simulated annealing. *Phys. Rev B*. **41**, 6335–6340.
[10] Du, Q., Gunzburger, M. D. & Peterson, J. S. (1992) Analysis and approximations of Ginzburg-Landau models for superconductivity. *SIAM Rev.* **34**, 54–81.
[11] Du, Q., Gunzburger, M. D. & Peterson, J. S. (1993) Modelling and analysis of a periodic Ginzburg-Landau model for type-II superconductors. *SIAM J. Appl. Math.* **53**, 689–717.

[12] Du, Q. (1994) Global existence and uniqueness of solutions of the time-dependent Ginzburg-Landau models for superconductivity. *Applicable Analysis.* **53**, 1–17.
[13] Du, Q. (1994) Finite element methods for the time-dependent Ginzburg-Landau model of superconductivity. *Comp. Math. Appl.* **27**, 119–133.
[14] Du, Q. (1996) Computational methods for the time-dependent Ginzburg-Landau model of superconductivity. In: Cai, W., Shi, C., Shu, C. and Xu, J. (eds.), *Numerical Methods for Applied Sciences.*New York. Science Press, pp. 51–65.
[15] Garner, J., Spanbauer, M., Benedek, R., Strandburg, K., Wright, S. & Plasmann, P. (1992) Critical fields of Josephson-coupled superconducting multilayers. *Phys. Rev. B*, **45**, 7973–7983.
[16] Galbreath, N., Grop, W., Gunter, D., Leaf, G. & Levine, D. (1993) Parallel solution of the three-dimensional time-dependent Ginzburg-Landau equation. *Proc. SIAM Conf. on Parallel Processing for Scientific Computing*. SIAM, Philadelphia.
[17] Gor'kov, Ld. (1959) Microscopic deviation of the Ginzburg–Landau equations in the theory of superconductivity. *Zh. Exsper. Teoret. Fiz* **36**, 1918–1923.
[18] Jones, M. T. & Plassmann, P. E. (19??) Computation of equilibrium vortex structures for type-II superconductors. *Int. J. Supercomput. Applic.* **7**(2), 129–143.
[19] Kaper, H. G. & Takac, P. (1997) An equivalence relation for the Ginzburg-Landau equations of superconductivity. *Z. Angew. Math. Phys.* **48**, 665–675.
[20] Kresin, V. Z. & Wolf, S. A. (1990) *Fundamentals of Superconductivity*. Plenum Press.
[21] Kuper, C. G. (1968) *An Introduction to the Theory of Superconductivity*. Clarendon Press.
[22] Kwong, M. K. & Kaper, H. G. (1995) Vortex configurations in type-II superconducting films. *J. Comput. Phys.* **119**, 120–131.
[23] Lin, F. & Du, Q. (1997) Ginzburg-Landau vortices: dynamics, pinning, and hysteresis. *Siam J. Math. Anal.* **28**, 1265–1293.
[24] Machida, M. & Kaburaki, H. (1993) Direct simulation of the time-dependent Ginzburg-Landau equation for type-II superconducting thin films. *Phys. Rev. Lett.* **71**.
[25] Tilley, D. R. & Tilley, J. (1986) *Superfluidity and superconductivity*. Adam Hilger.
[26] Tinkham, M. (1975) *Introduction to Superconductivity*. Krieger.
[27] Schmid, A. (1966) A time-dependent Ginzburg-Landau equation and its application to the problem of resistivity in the mixed state. *Phys. Kondens. Mater.* **5**, 302–317.
[28] Wang, Z. D. & Hu, C. R. (1991) A numerical relaxation approach for solving the general Ginzburg-Landau equations for type-II superconductors. *Phys. Rev. B*, **44**, 11918.